AJNR

Fluoroscopic MR of the pharynx in patients with obstructive sleep apnea.

L Jäger, E Günther, J Gauger and M Reiser

AJNR Am J Neuroradiol 1998, 19 (7) 1205-1214
http://www.ajnr.org/content/19/7/1205

AJNR Am J Neuroradiol 19:1205–1214, August 1998

Fluoroscopic MR of the Pharynx in Patients with Obstructive Sleep Apnea

Lorenz Jäger, Eck Günther, Jörg Gauger, and Maximilian Reiser

PURPOSE: **The purpose of our study was to introduce an ultrafast MR imaging technique of the pharynx as a diagnostic tool for viewing the mechanism of obstruction in patients with obstructive sleep apnea.**

METHODS: **Six healthy volunteers and 16 patients with obstructive sleep apnea were examined on a 1.5-T whole-body imager using a circular polarized head coil. Ultrafast two-dimensional fast low-angle shot sequences were obtained in midsagittal and axial projections during transnasal shallow respiration at rest, during simulation of snoring, and during performance of the Müller maneuver. All patients underwent physical examination, transnasal fiberoptic endoscopy, and polysomnography.**

RESULTS: **Five to six images were obtained per second with an in-plane resolution of 2.67 × 1.8 mm and 2.68 × 2.34 mm, allowing visualization of motion of the tongue, soft palate, uvula, and posterior pharyngeal surface. MR findings correlated well with results of clinical examination. The length of obstruction in the oropharynx, which cannot be ascertained by transnasal endoscopy of the pharynx, was clearly visible MR images. Differences between patients with obstructive sleep apnea and healthy subjects in terms of the degree of obstruction in the velopharynx and oropharynx depicted on MR images during the Müller maneuver were highly significant.**

CONCLUSION: **We believe that ultrafast MR imaging is a reliable noninvasive method for use in the evaluation of obstructive sleep apnea.**

Diagnosis and treatment of obstructive sleep apnea (OSA) are critical, since patients with OSA suffer from excessive daytime sleepiness, shortening of rapid eye movement sleep phases, daytime hypersomnolence, and gastroesophageal reflux. Cardiovascular derangements, such as hypertension, arrhythmias, ST depression, loss of circadian variation, and rise of blood pressure, are additional symptoms that may affect the individual's ability to work and possibly lead to a higher risk of stroke and myocardial infarction (1–12).

Several therapeutic approaches have been developed to treat OSA. These include continuous positive nasal airway pressure, uvulopalatopharyngoplasty, mandibular osteotomy/genioglossus advancement with hyoid myotomy/suspension, and maxillary and mandibular advancement osteotomy (3, 10, 13–15).

Recent advances in imaging techniques have fostered the development of new approaches for identification of the dynamic anatomy and physiology of the pharynx. The techniques available include cineradiography (16–20), CT (21, 22), ultrafast CT (18, 23–25), and MR imaging (26–28). Disadvantages associated with the use of cineradiography, CT, and ultrafast CT include exposure of the patient to X-rays and limited imaging planes. On the other hand, a major advantage of MR imaging is the feasibility of viewing the pharynx in multiple imaging planes without exposing the patient to ionizing radiation. The aim of this study was to evaluate the potential of fast MR imaging in the diagnosis of OSA.

Methods

Sixteen patients (mean age, 55 years [SD, ±11]; mean body mass index, 28 kg/m^2 [SD, ±3]) with daytime hypersomnolence and OSA were examined prospectively. A body mass index of lower than 25 kg/m^2 is within normal range, a body mass index between 25 and 29 kg/m^2 is above normal, and a body mass index of 30 and higher kg/m^2 is significantly above normal. No patient received any treatment before MR examination. Each patient underwent physical examination, transnasal fiberoptic endoscopy, and polysomnography.

Received September 10, 1996; accepted after revision January 22, 1998.

From the Departments of Radiology (L.J., J.G., M.R.) and ENT (E.G.), Institut für Radiologische Diagnostik, Klinikum Großhadern, Ludwig-Maximilians-Universität München, München, Germany.

Address reprint requests to Dr. Lorenz Jäger, Institut für Radiologische Diagnostik, Klinikum Großhadern, der Ludwig-Maximilians-Universität München, Marchioninistr. 15, 81366 München, Germany.

In all patients, obstructive apnea was diagnosed by standardized overnight polysomnography, including a two-channel electroencephalogram (C3, C4, references A1 and A2), a two-channel electrooculogram, a chin electromyogram, measurement of oronasal airflow with a thermistor, measurement of oxygen saturation (Sao_2) with pulse oximetry from a flexible finger probe, recording of snoring sounds with a neck microphone, an ECG, and recording of thoracic and abdominal respiratory movements with strain gauge thoracic and abdominal belts. In addition, leg movements were measured with a bilateral tibialis electromyogram.

Obstructive apnea was defined as a cessation of oronasal airflow lasting 10 seconds or longer, with respiratory efforts detected in the thoracoabdominal movement recordings, followed by a fall in Sao_2 of at least 4% within 30 seconds. Central apnea was defined as an event lasting 10 seconds or longer, with a combination of cessation of oronasal airflow and absence of thoracoabdominal breathing efforts. Mixed apnea was defined as an event lasting 10 seconds or more, with a beginning central apnea constituting at least 5 seconds of the total apneic episode, followed by an obstructive apneic event. Indexes of the different types of apnea (apnea index, apnea-hypopnea index) were calculated as the sum of hypopneic and apneic episodes per hour of sleep. Apart from the clinical findings, the polysomnographic criteria of apnea were met if the patient had an apnea index and apnea-hypopnea index above 10 per hour of sleep.

Before undergoing MR imaging, all patients had transnasal fiberoptic endoscopy in the supine position, during which the grade of narrowing of the velo- and oropharynx was estimated in percentage points during performance of the Müller maneuver at both levels. A narrowing of 30% or less was regarded as mild, a narrowing greater than 30% but less than 60% was regarded as moderately severe, and a narrowing of 60% or more was regarded as severe. The Müller maneuver consisted of an inspiratory effort with the mouth and nose closed (with a

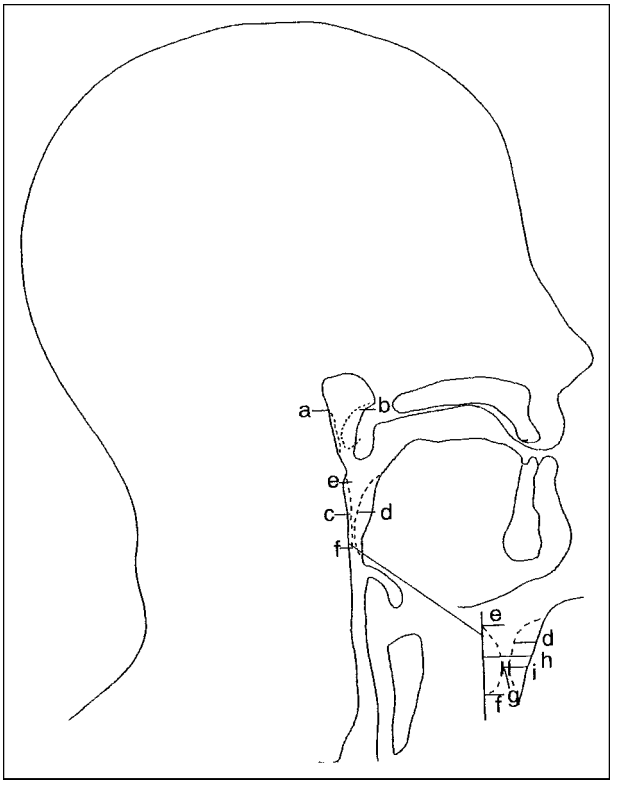

FIG 1. Midsagittal plane during simulation of snoring or during the Müller maneuver. *Dotted line* a = mobility of the posterior pharyngeal surface in the velopharynx; *dotted line* b = mobility of the uvula; *dotted line* c = mobility of the posterior pharyngeal surface in the oropharynx; *dotted line* d = mobility of the tongue base; distance between e and f = length of occlusion; i = mobility of the tongue base; h = luminal longitudinal diameter during shallow respiration; g = luminal longitudinal diameter during simulation of snoring or during the Müller maneuver.

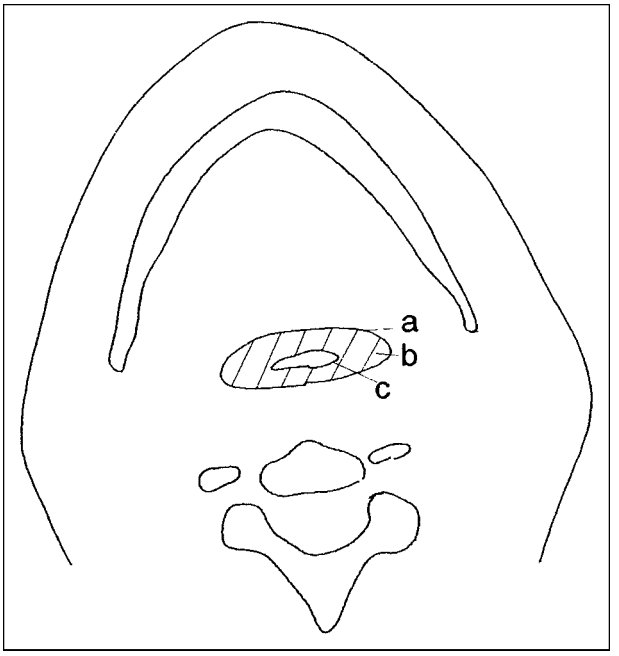

FIG 2. Occlusion of the oropharynx during simulation of snoring or during the Müller maneuver. a = luminal cross-sectional area during shallow respiration; b = occlusion during simulation of snoring or during the Müller maneuver; c = luminal cross-sectional area during simulation of snoring or during the Müller maneuver.

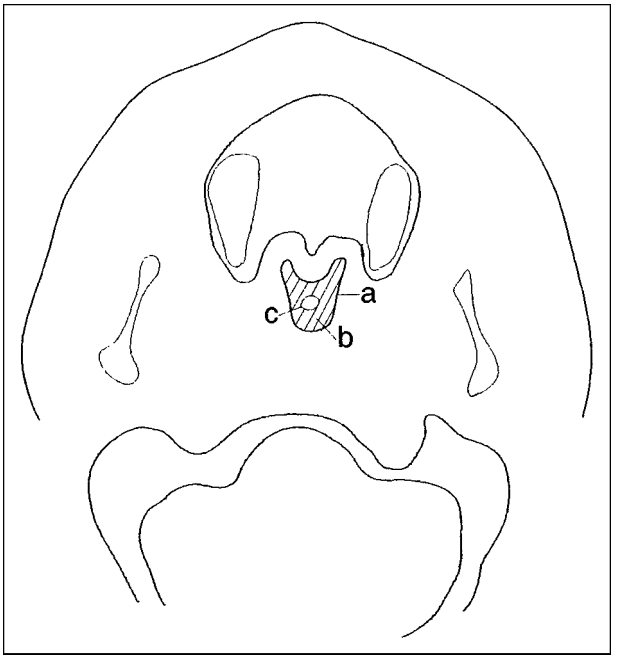

FIG 3. Occlusion of the velopharynx during simulation of snoring or during the Müller maneuver. a = luminal cross-sectional area during shallow respiration; b = occlusion during simulation of snoring or during the Müller maneuver; c = luminal cross-sectional area during simulation of snoring or during the Müller maneuver.

plastic clip). This respiratory maneuver produced a vacuum, which resulted in total or partial collapse of the pharyngeal surface.

The Müller maneuver was also performed during MR imaging. To estimate the collapse or narrowing of the pharynx, the mobility of the posterior pharyngeal wall of the pharynx was measured, as was the change in the total luminal cross-sectional area of the pharynx at the site of the most severe narrowing or occlusion. To estimate the narrowing of the pharynx on the midsagittal images, the luminal anteroposterior diameter of the pharynx was measured during shallow respiration, during simulation of snoring, and during the Müller maneuver in the velo- and oropharynx at the site of maximum narrowing. The percentage of obstruction was calculated by using the following formula:

$$1)\quad \left(\frac{\text{LSD under SR} - \text{LSD under MM or SS}}{\text{LSD under SR}}\right) \times 100 = \text{percentage of obstruction},$$

where LSD = luminal sagittal diameter, SR = shallow respiration, MM = Müller maneuver, and SS = simulation of snoring.

The mobility of the posterior pharyngeal wall was measured on midsagittal images at the site of maximum narrowing (Fig 1), using the posterior pharyngeal surface during shallow respiration as a baseline. From this baseline, elevation of the pharyngeal surface was measured during the Müller maneuver or during simulation of snoring. The length of the occlusion was also measured on the midsagittal images.

Because it is not possible to estimate the mobility of the entire pharyngeal surface on sagittal images, axial images were chosen. The velopharynx was defined as extending from the posterior surface of the soft palate to the lateral and posterior pharyngeal surface. Thus, the velopharynx is part of the nasopharynx and extends to the inferior edge of the soft palate. The oropharynx extends from the inferior surface of the soft palate to the tip of the epiglottis and the lateral and posterior pharyngeal surface. At the site of maximum narrowing of the velo- and oropharynx seen in the midsagittal plane during the Müller maneuver, the luminal change in the pharynx was calculated in the axial plane during shallow respiration, during the Müller maneuver, and during simulation of snoring. The borders of the luminal cross-sectional area of the oropharynx were the lateral and posterior pharyngeal wall and the surface of the tongue base (Fig 2). The borders of the velopharynx were the surface of the lateral and posterior pharyngeal wall and the posterior surface of the soft palate (Fig 3). To obtain a reliable luminal cross-sectional area under shallow respiration, the area was measured in five respiratory cycles and calculated as a mean value. If there was a narrowing or occlusion of the pharynx during shallow respiration, it was calculated in relation to the mean value of the three respiratory cycles with the maximum luminal cross-sectional area at this site. The change in the luminal cross-sectional area of the pharynx was calculated in relation to the pharynx during shallow respiration. The per-

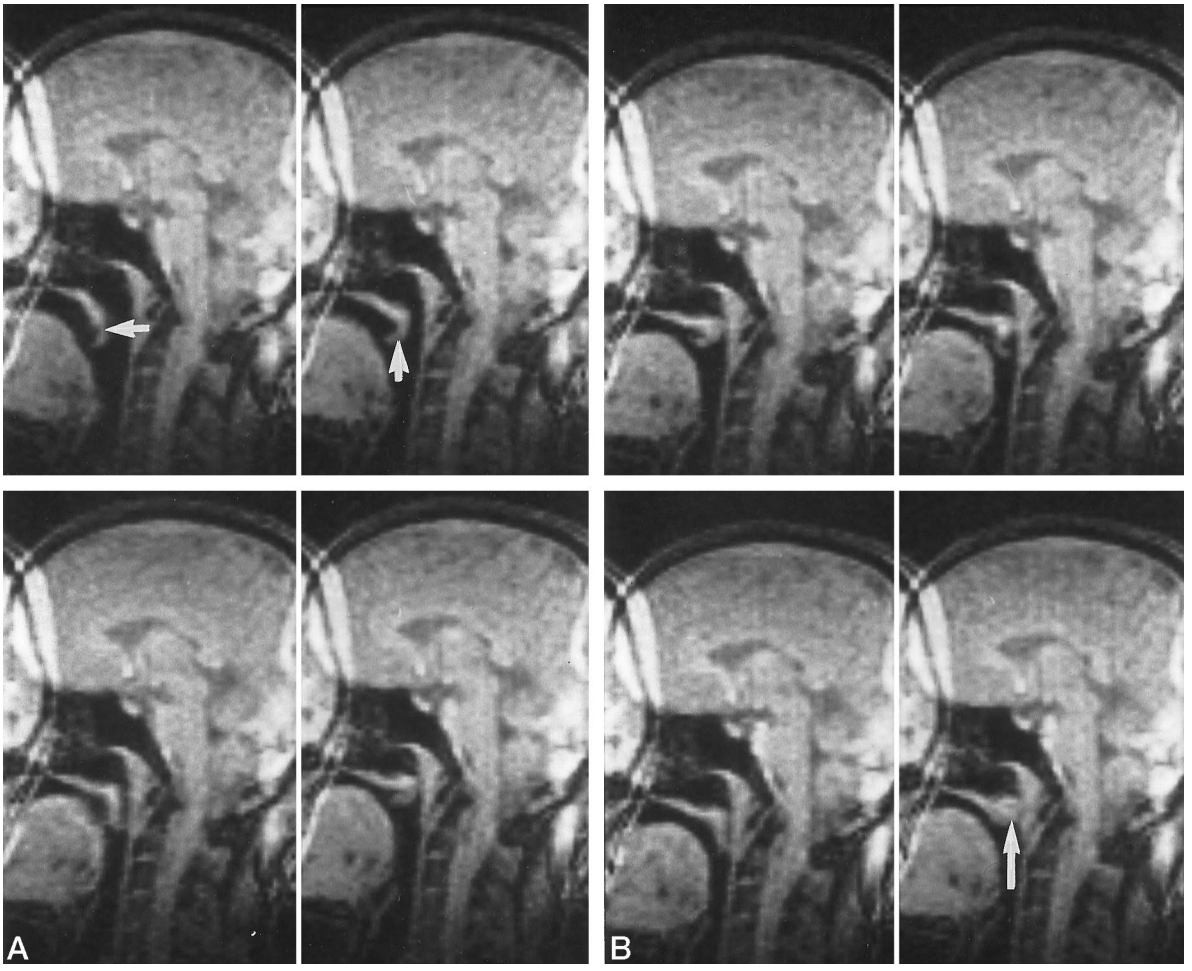

FIG 4. Patient with OSA. Spin density–weighted 2D-FLASH sequence.

A and *B*, Simulation of snoring, sagittal projection. Every second image is presented at an interval of 3.2 seconds. The motion of the uvula can be clearly detected (*short arrows*), and an obstruction of the velopharynx is seen (*long arrow*).

centage of occlusion of the pharynx was calculated by using the following formula:

$$2)\quad \left(\frac{\text{LCSA under SR} - \text{LCSA under MM or SS}}{\text{LCSA under SR}}\right) \times 100 = \text{percentage of obstruction,}$$

where LCSA = luminal cross-sectional area, SR = shallow respiration, MM = Müller maneuver, and SS = simulation of snoring. For all measurements, we used the evaluation software in the MR unit.

Because of the size constraints of the whole-body MR imager (a diameter of 45 cm), patients had to weigh less than 125 kg. Patients heavier than 125 kg usually did not fit into the magnet or, if they did, were unable to put the plastic clip on their nose, which was necessary for the Müller maneuver.

Six healthy volunteers (mean age, 28 years [SD, ±2]; body mass index, 20–28 kg/m^2 [SD, ±2] were also examined with MR imaging. These volunteers did not suffer from breathing problems, sleep disorders, or daytime fatigue. They had no history of snoring or acute or chronic upper respiratory tract diseases, nor were they currently taking hypnotic medication. All six control subjects also underwent transnasal fiberoptic endoscopy in the supine position while they performed the same respiratory maneuvers as the patients with OSA. The control subjects were defined as healthy if they did not show a narrowing or obstruction during endoscopy. Findings at MR imaging and transnasal fiberoptic endoscopy were compared between the volunteers and patients. All patients and volunteers gave informed written consent to the protocol that was approved by the institution's ethics commission.

MR imaging was performed with a 1.5-T whole-body unit using a circular polarized head coil. Midsagittal images of the pharynx were acquired using a spin density–weighted two-dimensional fast low-angle shot (2D-FLASH) sequence with imaging parameters of 3.5/1.7 (TR/TE), a flip angle of 8°, a 5-mm section thickness, a 56 × 128 matrix, and a 150 × 300 mm field of view; six images were acquired per second. Axial sections of the velo- and oropharynx were acquired using a 2D-FLASH sequence with imaging parameters of 4.5/2.2, a flip angle of 8°, a 5-mm section thickness, a 43 × 128 matrix, and a 125 × 230-mm field of view; five images were acquired per second. The total in-plane resolution varied between 2.68 × 2.34 mm and 2.67 × 1.80 mm. Each section location was imaged 60 consecutive times, with a total acquisition time of 10 to 13 seconds. During MR imaging, the subjects were instructed to perform transnasal shallow respiration at rest without swallowing while the mouth was closed, then a simulation of snoring and a Müller maneuver were performed. The sagittal images were acquired first. Subsequently, the axial imaging projections were planned in the velo- and oropharynx at the site of maximum pharyngeal narrowing during the Müller maneuver. The patients did not receive paramagnetic contrast agents or sedation, and they were fully awake during the entire procedure.

Because the data were not normally distributed (Shapiro-Wilk test), nonparametric statistical methods were used. Differences between the two groups were assessed with the Mann-Whitney *U* test, and correlations between variables were calculated with the Spearman rank correlation test. The .05 level of confidence was selected as indicating statistical significance. The level of .01 was interpreted as very significant and .005 as highly significant.

Results

With our MR protocol, dynamic imaging of the pharynx was performed with good air/soft tissue contrast without the use of any paramagnetic contrast medium. The different phases of tongue movement,

TABLE 1: Evaluation of respiratory maneuvers with MR (percentage of pharyngeal occlusion)

Patient	N/V sag	S/V sag	M/V sag	N/O sag	S/O sag	M/O sag	N/V ax	S/V ax	M/V ax	N/O ax	S/O ax	M/O ax
1	0	0	0	0	0	0	0	100	100	0	0	50
2	0	100	100	0	0	0	0	100	100	0	0	50
3	0	100	100	0	0	100	0	100	89	0	45	100
4	100	100	100	0	0	50	100	100	100	0	20	100
5	0	100	100	0	0	80	0	0	100	0	0	80
6	0	0	0	0	60	60	0	30	100	0	50	100
7	0	100	100	60	100	0	50	100	100	60	100	100
8	0	0	75	100	100	100	0	77	77	33	100	100
9	0	20	100	0	100	100	0	20	100	0	100	100
10	0	0	0	0	100	100	0	0	50	40	68	100
11	0	0	0	0	75	100	0	50	50	40	40	100
12	0	0	23	0	80	100	0	0	50	0	50	100
13	0	0	50	0	40	100	0	0	50	0	100	100
14	0	0	80	100	100	100	0	80	30	100	100	100
15	0	100	100	100	100	100	0	100	100	100	100	100
16	0	0	100	0	50	100	0	50	100	0	75	100
Mean values ± SD	6.25 ± 24.21	38.75 ± 47.68	64.25 ± 42.577	22.50 ± 39.92	56.56 ± 42.23	81 ± 24.72	9.38 ± 26.33	56.69 ± 41.241	81 ± 24.72	23.31 ± 34.64	59.25 ± 38.00	91.25 ± 16.91

Note.—N, transnasal shallow respiration at rest; M, Müller maneuver; S, simulation of snoring; V, velopharynx; O, oropharynx; ax, axial; sag, sagittal.

the elevation of the uvula, and the mobility of the soft tissue of the pharyngeal surface of the velo- and oropharynx were visible on MR images in both healthy volunteers and patients with OSA while they simulated snoring or performed the Müller maneuver (Fig 4–8). Pharyngeal narrowing or obstruction did not occur at particular times but occurred randomly during the respiratory maneuvers.

The most severe occlusion of the oropharynx was detected during the Müller maneuver in patients 6, 8, 11, 12, 13, and 14, with a longitudinal extension of 3 cm, 6 cm, 3 cm, 2 cm, 2.5 cm, and 3 cm, respectively, on the midsagittal images. The greatest mobility of the posterior pharyngeal surface was detected in patients 11 (1.5 cm) and 13 (1 cm). Ultrafast MR imaging depicted the extent of oropharyngeal obstruction more distinctly than did endoscopy, because endoscopy did not enable an evaluation of the length of the occlusion. The degree of obstruction of the oropharynx was estimated to be smaller at endoscopy than at MR imaging in the seven of 16 patients who performed the Müller maneuver (Fig 9). During transnasal shallow respiration at rest, a narrowing of the velopharynx was observed in patient 4 and of the oropharynx in patients 7, 8, 14, and 15 (Table 1).

In patients with OSA, obstruction of the velo- and oropharynx as detected on sagittal projections correlated well with the same occlusion detected on axial projections during performance of the Müller maneuver. In addition, highly significant correlations were observed between MR findings and findings at transnasal fiberoptic endoscopy in the axial projections of the velo- and oropharynx in these patients (Table 1–3). A significant correlation was found in the axial projection between MR images obtained during simulation of snoring and fiberoptic endoscopy during performance of the Müller

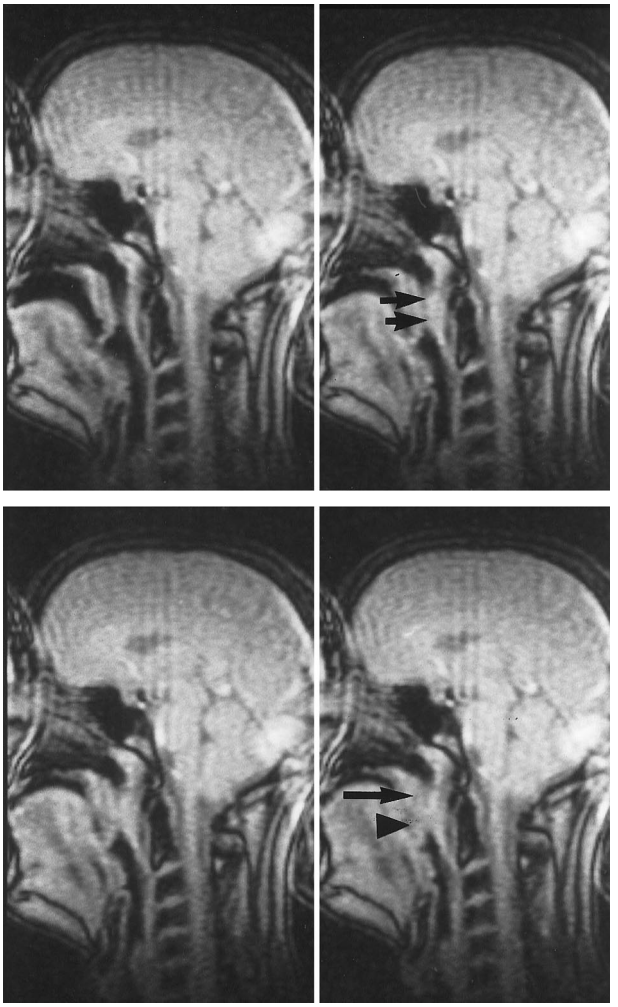

FIG 5. Patient with OSA. Spin density–weighted 2D-FLASH sequence. Müller maneuver, sagittal projection. Every fourth image is presented at an interval of 3.2 seconds. The motion of the tongue, uvula, and posterior pharyngeal surface (*short arrows*) can be delineated. An obstruction of the velopharynx (*long arrow*) and the oropharynx (*arrowhead*) is shown. The obstruction of the oropharynx is caused by a constriction of the uvula between the tongue and the posterior pharyngeal surface.

TABLE 2: Evaluation of the Müller maneuver with transnasal fiberoptic endoscopy in patients with OSA (percentage of pharyngeal occlusion)

Patients	Velopharynx	Oropharynx	AHI
P1	100	20	42
P2	100	30	18
P3	100	80	14
P4	100	100	31
P5	100	80	30
P6	100	100	46
P7	75	75	19
P8	100	100	52
P9	100	100	29
P10	75	95	45
P11	50	100	30
P12	50	100	42
P13	50	75	17
P14	90	80	38
P15	100	100	58
P16	100	100	35
Mean values ± SD	86.88 ± 20.16	83.44 ± 25.01	34.13 ± 13.03

Note.—AHI, apnea-hypopnea index.

TABLE 3: Correlation of different respiratory maneuvers and examination techniques in patients with OSA

Respiratory Maneuver and Examination Technique	*r*	*P*
MR-V-sag-M/MR-V-ax-M	.711	.006
MR-O-sag-M/MR-O-ax-M	.720	.005
MR-V-ax-M/Endo-V-ax-M	.826	.001
MR-O-ax-M/Endo-O-ax-M	.802	.002
MR-V-ax-S/Endo-V-ax-S	.595	.021
MR-V-sag-S/MR-V-sag-M	.842	.001
MR-O-sag-S/MR-O-sag-M	.587	.023
MR-V-ax-S/MR-V-ax-M	.632	.126
MR-O-ax-S/MR-O-ax-M	.616	.017

Note.—Endo, transnasal fiberoptic endoscopy; V, velopharynx; O, oropharynx; ax, axial; sag, sagittal; M, Müller maneuver; S, simulation of snoring.

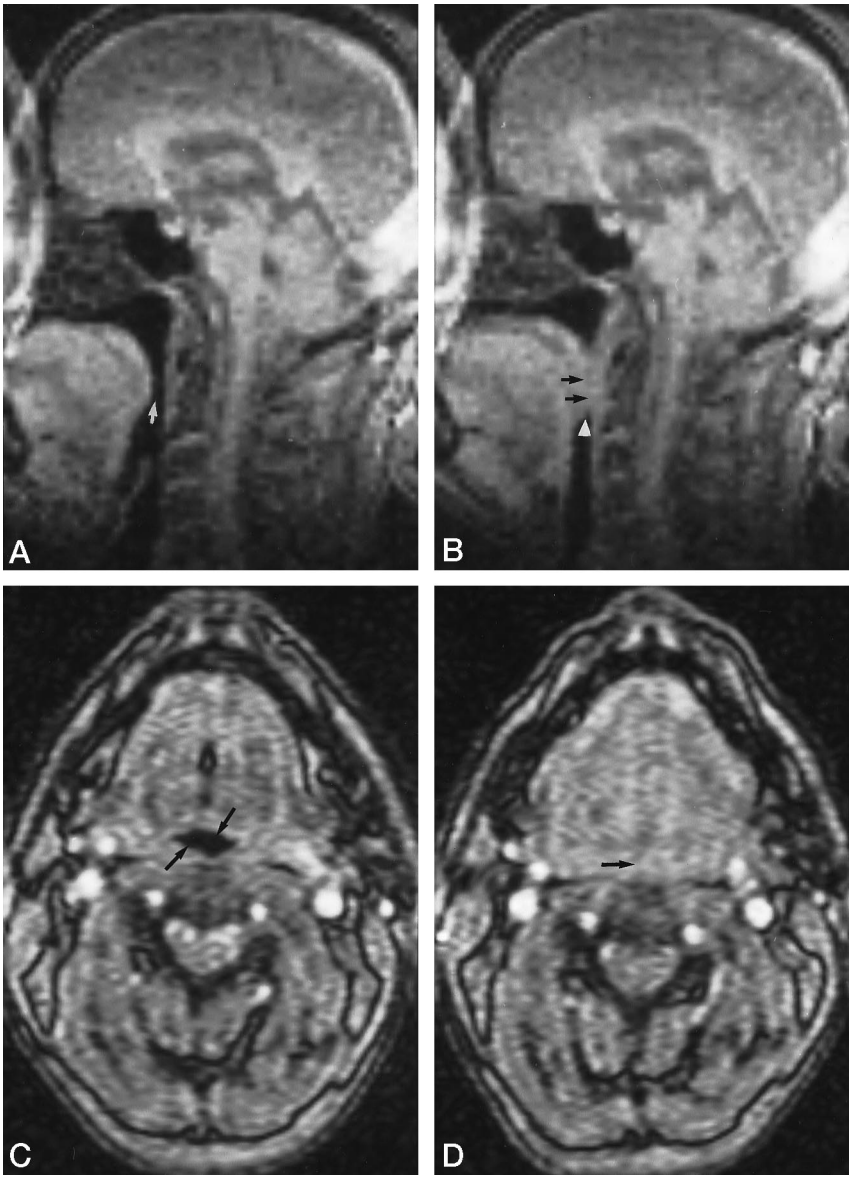

FIG 6. Patient with OSA. Spin density–weighted 2D-FLASH sequence.

A, Transnasal shallow respiration at rest, sagittal projection, shows no narrowing of the pharynx (*arrow*).

B, Müller maneuver, sagittal projection, shows increased mobility of the posterior pharyngeal surface (*arrows*) and obstruction of the oropharynx (*arrowhead*).

C, Transnasal shallow respiration at rest, axial projection, shows no obstruction of the oropharynx (*arrows*).

D, Müller maneuver, axial projection, shows an obstruction of the oropharynx (*arrow*).

maneuver in the velopharynx (Table 3); no significant correlations were observed for the oropharynx. For both respiratory maneuvers (simulation of snoring and Müller maneuver), significant correlations were observed in the velo- and oropharynx (Table 3; Figs 9 and 10). Contrary to the findings in the patients with OSA, neither severe narrowing of the pharynx nor soft tissue motion of the pharyngeal walls was detected in the healthy volunteers (Fig 11), with two exceptions (Table 4). One volunteer sustained an obstruction of 77% in the velopharynx on the sagittal projection while he was simulating snoring; another sustained an obstruction of 85% in the velopharynx on the sagittal images while he was performing the Müller maneuver. In both subjects, the narrowing was caused by a relapse of the uvula into the velopharynx. This severe narrowing could not be confirmed with the other respiratory or imaging techniques.

The differences in the degree of obstruction on the axial projections between patients with OSA and healthy subjects was highly significant for the Müller maneuver and for the simulation of snoring in the velo- and oropharynx (Table 5).

In patients with OSA, we could not find any significant correlation between the MR results and the apnea-hypopnea index measured during polysomnography. However, a significant correlation was observed between this index and the endoscopic findings in the oropharynx ($r = .585$, $P = .0236$).

Discussion

Patients with OSA have an increased mobility of soft tissue in the velo- and oropharynx, which results in recurrent obstruction of the pharyngeal airway and the intermittent cessation of breathing. Analyses of the pharynx in patients with OSA have been per-

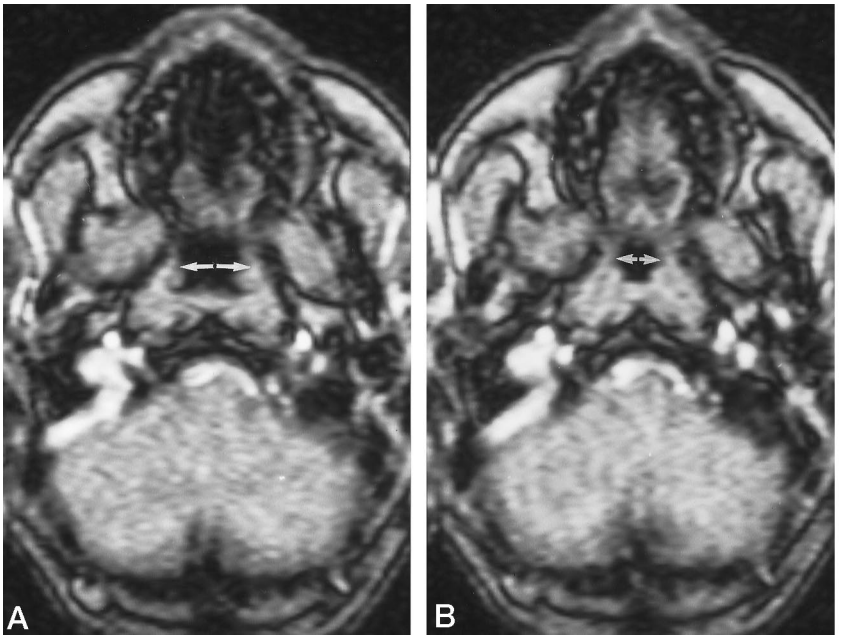

FIG 7. Patient with OSA. Spin density–weighted 2D-FLASH sequence.
A, Transnasal shallow respiration at rest, axial projection, shows no narrowing of the velopharynx (*arrows*).
B, Müller maneuver, axial projection, shows a narrowing of the velopharynx but no obstruction (*arrows*).

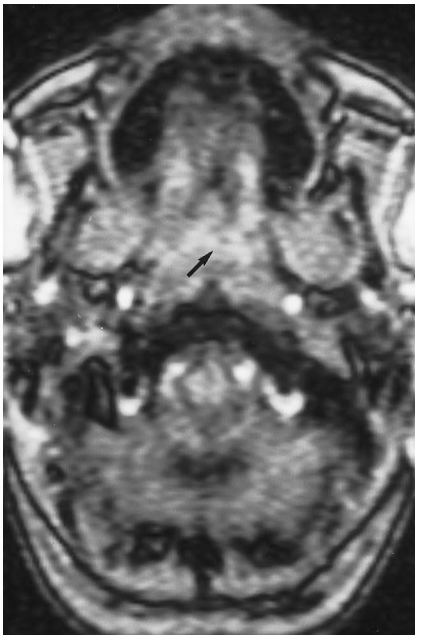

FIG 8. Patient with OSA. Spin density–weighted 2D-FLASH sequence. Müller maneuver, axial projection, shows an obstruction of the velopharynx (*arrow*).

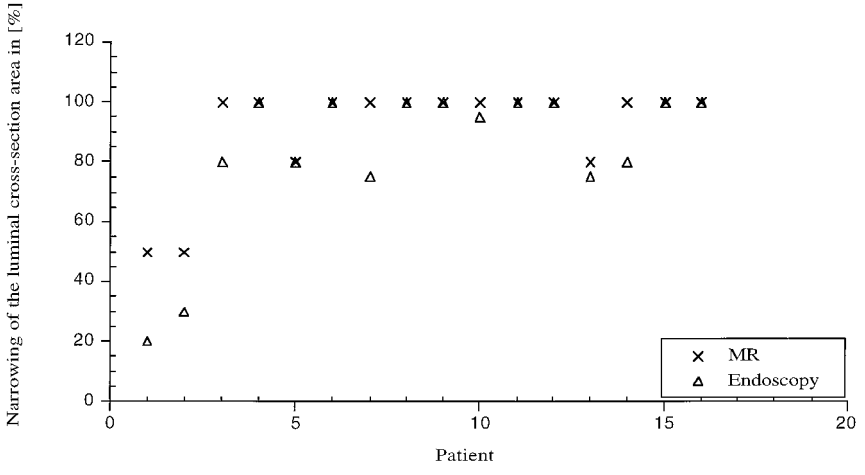

FIG 9. Occlusion of the oropharynx in patients with OSA during performance of the Müller maneuver.

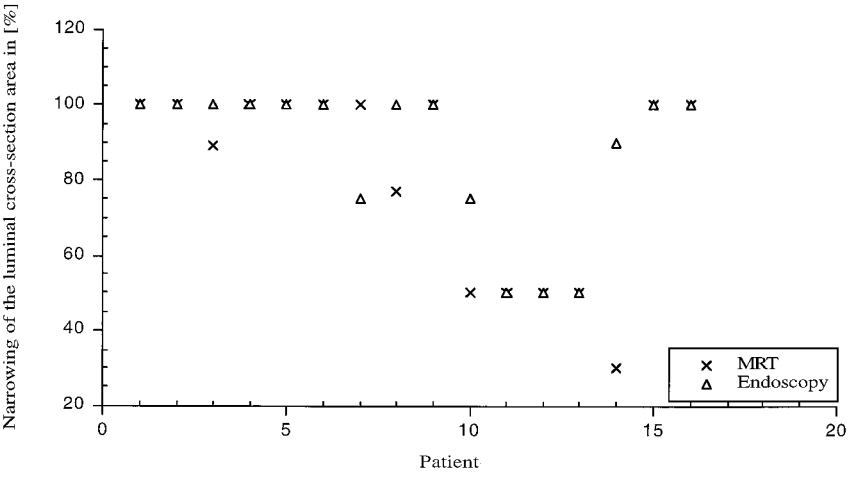

FIG 10. Occlusion of the velopharynx in patients with OSA during performance of the Müller maneuver.

FIG 11. Healthy volunteer. Spin density–weighted 2D-FLASH sequence, sagittal projection, during Müller maneuver, shows no narrowing of the pharynx (*arrow*).

formed with CT (18, 23–25), ultrafast CT (21, 22), and MR imaging (27–31).

The aim of these studies was to examine the volume and functional abnormalities of the pharynx in relation to the results of polysomnography and different therapeutic techniques. The results are inconsistent. The findings of some studies show the pharyngeal volume to be smaller in patients with OSA than in healthy control subjects (18, 25, 29). By contrast, other studies have reported that the mobility of the pharyngeal surface, and not the total volume of the pharynx, is responsible for occlusion of the upper airway and apnea (26, 30). On the basis of these findings, research shifted to dynamic imaging analyses of the pharynx with ultrafast CT (25) and fast MR sequences (27, 28, 29, 31, 32). The major advantage of ultrafast CT is good temporal resolution with an acquisition time of about 50 to 100 milliseconds. However, two major disadvantages of ultrafast CT include the exposure of patients to ionizing radiation and the inability to obtain primary images in the midsagittal or oblique plane. In addition, the axial and coronal scans must be reformatted to receive sagittal projections, with the limitation of decreased soft tissue contrast.

Fast MR imaging has been performed using gradient-recalled acquisition in the steady state (27, 28) and FLASH (32) sequences with an acquisition time of about 1 second per image, an in-plane resolution of about 2 mm, and a section thickness of 10 mm. However, fast MR imaging is still inadequate in terms of temporal resolution and section thickness. One MR study of speech mechanisms achieved a temporal resolution of three images per second, which is still too slow for imaging the mobility of the pharyngeal surface (31). Therefore, we implemented an ultrafast 2D-FLASH sequence with a temporal resolution of 5 images per second and reduced the section thickness to 5 mm. The temporal and in-plane resolution of this imaging technique proved to be reliable in the examination of OSA, since there was a highly significant correlation between findings with our MR technique and those obtained the well-established transnasal fiberoptic endoscopy of the pharynx. Furthermore, with this new technique, good air/soft tissue contrast, which is needed to delineate the pharyngeal surface, was obtained without intravenous administration of paramagnetic contrast material.

Although sagittal images have been used to show the sites and the vertical extension of narrowing and occlusion along the pharyngeal tube in patients with OSA, axial images are essential, because the midsagittal projection can only show the mobility of the posterior pharyngeal wall, the tongue base, and the uvula on sections with a thickness of 5 mm. Also, the axial projection is necessary to evaluate the mobility of the lateral pharyngeal walls and to examine the luminal cross-sectional area of the pharynx.

In contrast to published reports proposing that transnasal shallow breathing with its alternating airway pressure is sufficient to suggest the site of pharyngeal narrowing or obstruction (18, 25, 28, 29), our results have shown clearly that this is not the case. However, the Müller maneuver can indicate potential obstruction in the awake patient with OSA. In our study, the healthy control group, unlike the patients with OSA, did not sustain any severe changes or obstructions along the pharyngeal airway, with two exceptions. In these two subjects, a severe narrowing was detected only in the sagittal projection of the velopharynx during the simulation of snoring or during the Müller maneuver. There are two possible explanations for this occurrence. First, these were two healthy young adults who, in comparison with patients suffering from OSA, are more likely to be able to hyperextend the neck, which may facilitate the narrowing of the velopharynx by a relapse of the uvula during a forced respiratory maneuver. Second, the respiratory maneuver could have been performed with too much effort, resulting in an exaggerated narrowing of the velopharynx. To avoid a misinterpretation of the MR examination, imaging in two planes (sagittal and axial) and during at least two respiratory exercises (simulation of snoring and performance of the Müller maneuver) is needed to increase the probability that the patient is executing the respiration maneuver correctly during the examination.

The significant correlation between the findings at dynamic MR imaging and those at transnasal fiberoptic endoscopy shows that it is possible to detect the site of pharyngeal narrowing and occlusion with functional ultrafast MR imaging in awake patients. In contrast to a previous study (32), we did not perform imaging on sedated patients or volunteers, for two reasons. First, we think there is an increased risk of complications under sedation, such as obstruction of the upper airway by pharyngeal collapse or a relapse of the tongue if the

TABLE 4: Evaluation of respiratory maneuvers with MR (percentage of pharyngeal occlusion)

Volunteer	N/V sag	S/V sag	M/V sag	N/O sag	S/O sag	M/O sag	N/V ax	S/V ax	M/V ax	N/O ax	S/O ax	M/O ax
1	0	77	0	0	0	0	0	20	20	0	0	0
2	0	0	0	0	0	0	0	0	0	0	0	0
3	0	0	0	0	0	0	0	0	0	0	0	0
4	0	0	0	0	0	0	0	0	0	0	0	0
5	0	0	85	0	0	20	0	0	38	0	0	20
6	0	0	0	0	38	0	0	50	0	0	0	50
Mean values ± SD	0 ± 0	12.83 ± 28.70	14.17 ± 31.68	0 ± 0	6.33 ± 14.16	3.33 ± 7.45	0 ± 0	11.67 ± 18.63	9.67 ± 14.63	0 ± 0	0 ± 0	11.67 ± 18.63

Note.—N, transnasal shallow respiration at rest; M, Müller maneuver; S, simulation of snoring; V, velopharynx; O, oropharynx; ax, axial; sag, sagittal.

TABLE 5: Comparison of soft tissue mobility of the pharynx with MR in patients and volunteers during the Müller maneuver and simulation of snoring

Technique of Investigation	V-sag-M	O-sag-M	V-sag-S	V-sag-S	V-ax-M	O-ax-M	V-ax-S	O-ax-S
*P**	.0223	.0057	.2532	.0245	.0004	.0005	.0356	.004

Note.—V, velopharynx; O, oropharynx; ax, axial; sag, sagittal; M, Müller maneuver; S, simulation of snoring.

* Patients with OSA had a significantly higher ($P < .05$) mobility of the pharyngeal surface.

patient has lost his reflexes. Second, normal muscular tonus is lost under sedation and might increase the risk of pharyngeal occlusion.

Conclusion

Our results strongly suggest that ultrafast MR imaging is an objective and reliable method for investigating the pathogenetic mechanism of OSA, primarily because it is a noninvasive technique. Transnasal fiberoptic endoscopy of the pharynx, which is a well-established and accepted diagnostic tool for OSA (33, 34), seems to be more susceptible than MR imaging to underestimating the narrowing of the oropharynx. Furthermore, transnasal fiberoptic endoscopy does not allow for the measurement of the length of narrowing and obstruction of the pharynx. Instead, it requires a subjective estimation that is dependent on the training level of the examiner. These same measurements, however, are easily accomplished with MR imaging. Interestingly, the MR results and some of the endoscopic results did not correlate with the apnea-hypopnea index. Consequently, the Müller maneuver and the simulation of snoring seem to be valuable in detecting the site of obstruction but they cannot predict the apnea-hypopnea index value. Since the correlation between endoscopic findings and MR appearance during simulation of snoring is not as significant as endoscopic findings and MR appearance during the Müller maneuver, the Müller maneuver should be the respiratory exercise of choice.

Nevertheless, since the pathogenic mechanism of OSA has not yet been identified, modern MR techniques hold promise and play a critical role in the development of more detailed diagnoses that will facilitate the planning and monitoring of selective individual therapy.

Acknowledgment

We thank Laurie Gauger for reading and reviewing the manuscript.

References

1. Ferini-Strambi L, Zucconi M, Oldani A, et al. **Heart rate variability during sleep in snorers with and without obstructive sleep apnea.** *Chest* 1992;102:1023–1027
2. Gislason T, Benediktsdottir B, Bjornsson J, et al. **Snoring, hypertension, and the sleep apnea syndrome: an epidemiologic survey of middle-aged women.** *Chest* 1993;103:1147–1151
3. Hanly P, Sasson Z, Zuberi N, et al. **Ventricular function in snorers and patients with obstructive sleep apnea.** *Chest* 1992;102:100–105
4. Haraldson PO, Carenfelt C, Tingvall C. **Sleep apnea syndrome and automobile driving in a general population.** *J Clin Epidemiol* 1992; 45:821–825
5. Koskenvuo M, Kaprio J, Telakivi T, et al. **Snoring as a risk factor for ischaemic heart disease and stroke in men.** *BMJ* 1987;294: 16–19
6. Mateika JH, Mateika S, Slutsky AS, et al. **The effect of snoring on mean arterial blood pressure during non-REM sleep.** *Am Rev Respir Dis* 1992;145:141–146
7. Mendelson WB. **Sleepiness and hypertension in obstructive sleep apnea.** *Chest* 1992;101:903–909
8. Peter JH, Faust M. **Schlafbezogene Atemstörungen: Von den Syndromen zum Risikofaktor.** *Pneumologie* 1991;45:200–204
9. Rauscher H, Popp W, Zwick H. **Systemic hypertension in snorers with and without sleep apnea.** *Chest* 1992;102:367–371
10. Riley RW, Powell NB, Guilleminault C. **Obstructive sleep apnea syndrome: a review of 306 consecutively treated surgical patients.** *Otolaryngol Head Neck Surg* 1993;108:117–125
11. Smirne S, Palazzi S, Zucconi M, et al. **Habitual snoring as a risk factor for acute vascular disease.** *Eur Respir J* 1993;6:1357–1361
12. Spriggs D, French JM, Murdy J, et al. **Snoring increases the risk of stroke and adversely affects prognosis.** *Q J Med* 1992;83:555–562
13. Brown IB, McClean PA, Boucher R, et al. **Changes in pharyngeal cross-sectional area with posture and application of continuous positive airway pressure in patients with obstructive sleep apnea.** *Am Rev Respir Dis* 1987;136:628–632
14. Fleetham JA. **Upper airway imaging in relation to obstructive sleep apnea.** *Clin Chest Med* 1992;13:399–416
15. Sulsenti G, Palma P. **Carbon dioxide laser uvulopalatopharyngoplasty (UPPP).** *Acta Otorhinolaryngol Ital* 1993;13:53–62

16. Hess U, Hannig C, Sander S, et al. **Objective rendering of velopharyngeal closure in cleft patients with high-frequency-cineradiography.** *Eur Radiol* 1995;5(suppl):256
17. Pepin JL, Ferretti G, Veale D, et al. **Somnofluoroscopy, computed tomography, and cephalometry in the assessment of the airway in obstructive sleep apnea.** *Thorax* 1992;47:150–156
18. Stein MG, Gamsu G, de Geer G, et al. **Cine CT in obstructive sleep apnea.** *AJR Am J Roentgenol* 1987;148:1069–1074
19. Mahlo HW, Hannig C, Wuttge-Hannig A. **Roentgen cinematographic studies in patients who snore.** *Laryngol Rhinol Otol* 1988; 67:446–448
20. Suratt PM, Dee P, Atkinson RL, et al. **Fluoroscopic and computed tomographic features of the pharyngeal airway in obstructive sleep apnea.** *Am Rev Respir Dis* 1983;127:487–492
21. Ryan CF, Lowe AA, Li D, et al. **Three-dimensional upper airway computed tomography in obstructive sleep apnea.** *Am Rev Respir Dis* 1991;144: 428–432
22. Avrahami E, Englender M. **Relation between CT axial cross-sectional area of the oropharynx and obstructive sleep apnea syndrome in adults.** *AJNR Am J Neuroradiol* 1995;16:135–140
23. Brasch RC, Gould RG, Gooding CA, et al. **Upper airway obstruction in infants and children: evaluation with ultrafast CT.** *Pediatr Radiol* 1987;165:459–466
24. Ergun GA, Kahrilas PJ, Lin S, et al. **Shape, volume, and content of the deglutitive pharyngeal chamber imaged by ultrafast computerized tomography.** *Gastroenterology* 1993;105:1396–1403
25. Galvin JR, Rooholamini SA, Stanford W. **Obstructive sleep apnea: diagnosis with ultrafast CT.** *Radiology* 1989;171:775–778
26. Abbey NC, Block AJ, Green D, et al. **Measurement of pharyngeal volume by digitized magnetic resonance imaging.** *Am Rev Respir Dis* 1989;140:717–723
27. Shellock FG, Schatz CJ, Julien PM et al. **Dynamic study of the upper airway with ultrafast spoiled GRASS MR imaging.** *J Magn Reson Imaging* 1992;2:103–107
28. Shellock FG, Schatz CJ, Julien PM, et al. **Occlusion and narrowing of the pharyngeal airway in obstructive sleep apnea: evaluation by ultrafast spoiled GRASS MR imaging.** *AJR Am J Roentgenol* 1992; 158:1019–1024
29. Ryan CF, Lowe AA, Li D, et al. **Magnetic resonance imaging of the upper airway in obstructive sleep apnea before and after chronic nasal continuous positive airway pressure therapy.** *Am Rev Respir Dis* 1991;144:939–944
30. Suratt PM, Dee P, Atkinson RL, et al. **Fluoroscopic and computed tomographic features of the pharyngeal airway in obstructive sleep apnea.** *Am Rev Respir Dis* 1983;127:487–492
31. Hagen R, Haase A, Matthaei D, et al. **Oropharyngeale Funktionsdiagnostik mit der FLASH-MR-Tomographie.** *HNO* 1990;38: 421–425
32. Suto Y, Matsuo T, Kato T, et al. **Evaluation of the pharyngeal airway in patients with sleep apnea: value of ultrafast MR imaging.** *AJR Am J Roentgenol* 1993;160:311–314
33. Sher AE, Thorpy MJ, Spielmann AJ, et al. **Predictive value of Müller maneuver in selection of patients for uvulopalatopharyngoplasty.** *Laryngoscope* 1985;95:1483–1487
34. Sher AE. **Obstructive sleep apnea: diagnosis by history, physical examination and special studies. In: Fairbanks DNF, Fujita J, eds.** *Snoring and Obstructive Sleep Apnea*. New York: Raven Press; 1994:17–29